

# Galaxy Formation and Evolution

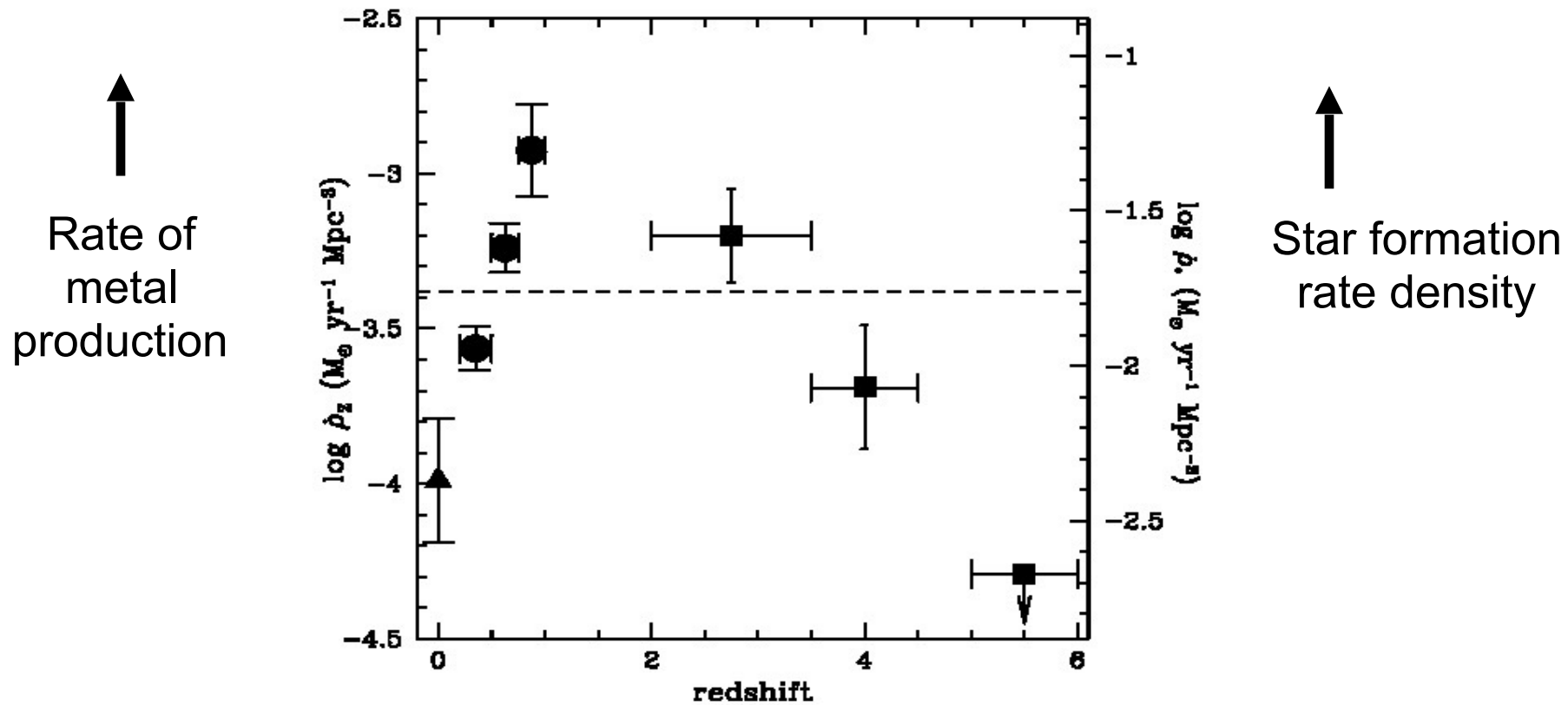
## Lecture 07:

### The Madau Diagram & Lyman Break galaxies

# Course contents

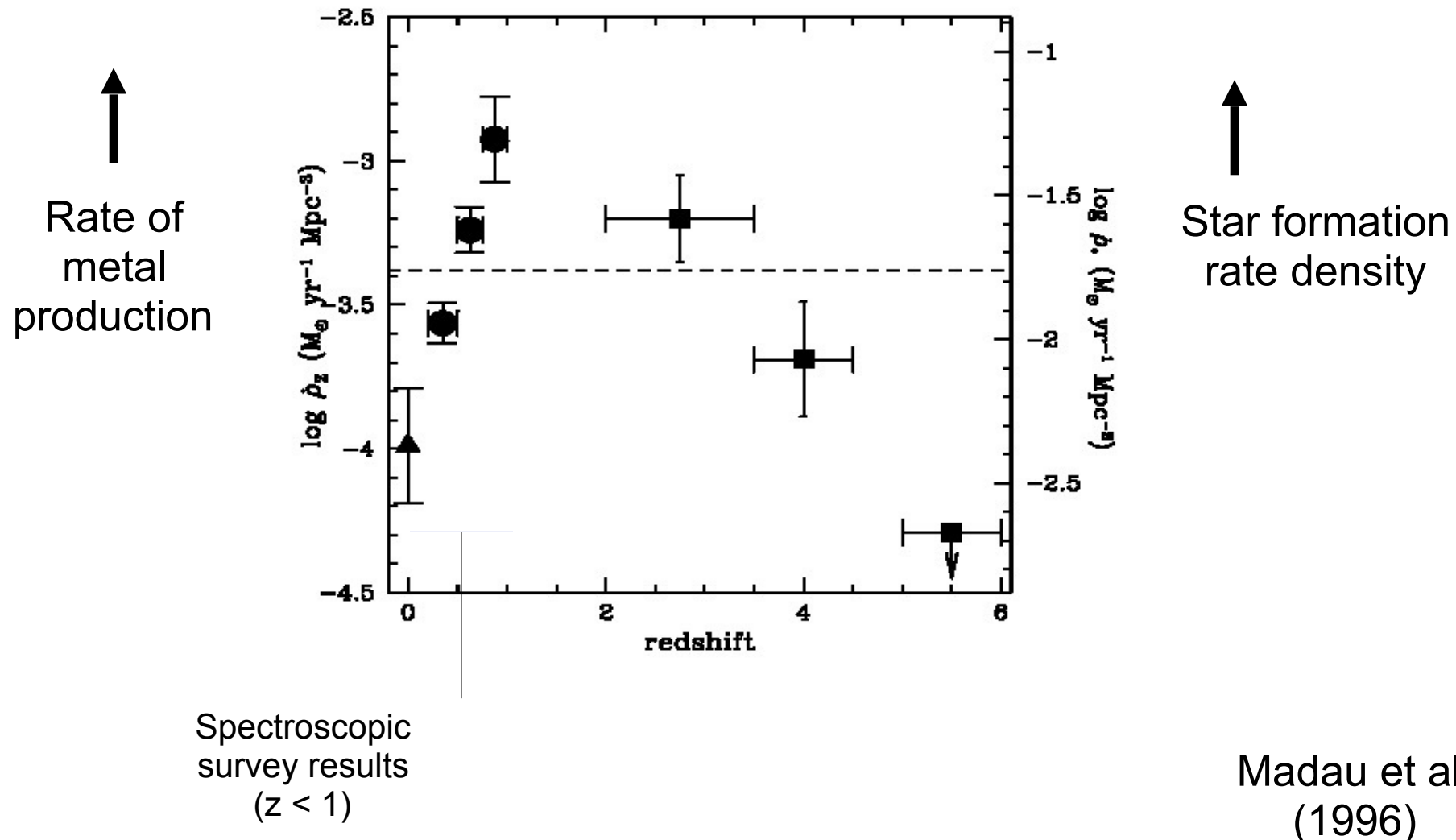
1. Historical introduction
2. Challenges and recent advances
3. Galaxy formation in theory
4. Spectral synthesis and star formation indicators
5. The fossil record for local galaxies
6. Survey astronomy
7. The Madau Diagram and Lyman Break galaxies
8. Studying galaxy evolution in the IR/sub-mm
9. The evolution of early-type galaxies
10. Morphological evolution and spiral galaxies
11. AGN discovery and observed properties
12. AGNs and supermassive black holes
13. Black hole growth and formation
14. The triggering of AGN
15. AGN feedback and outflows
16. The link between star formation and AGN activity
17. The far frontier and outstanding challenges
18. The future of the Universe

# The star formation history of the Universe: the “Madau diagram”

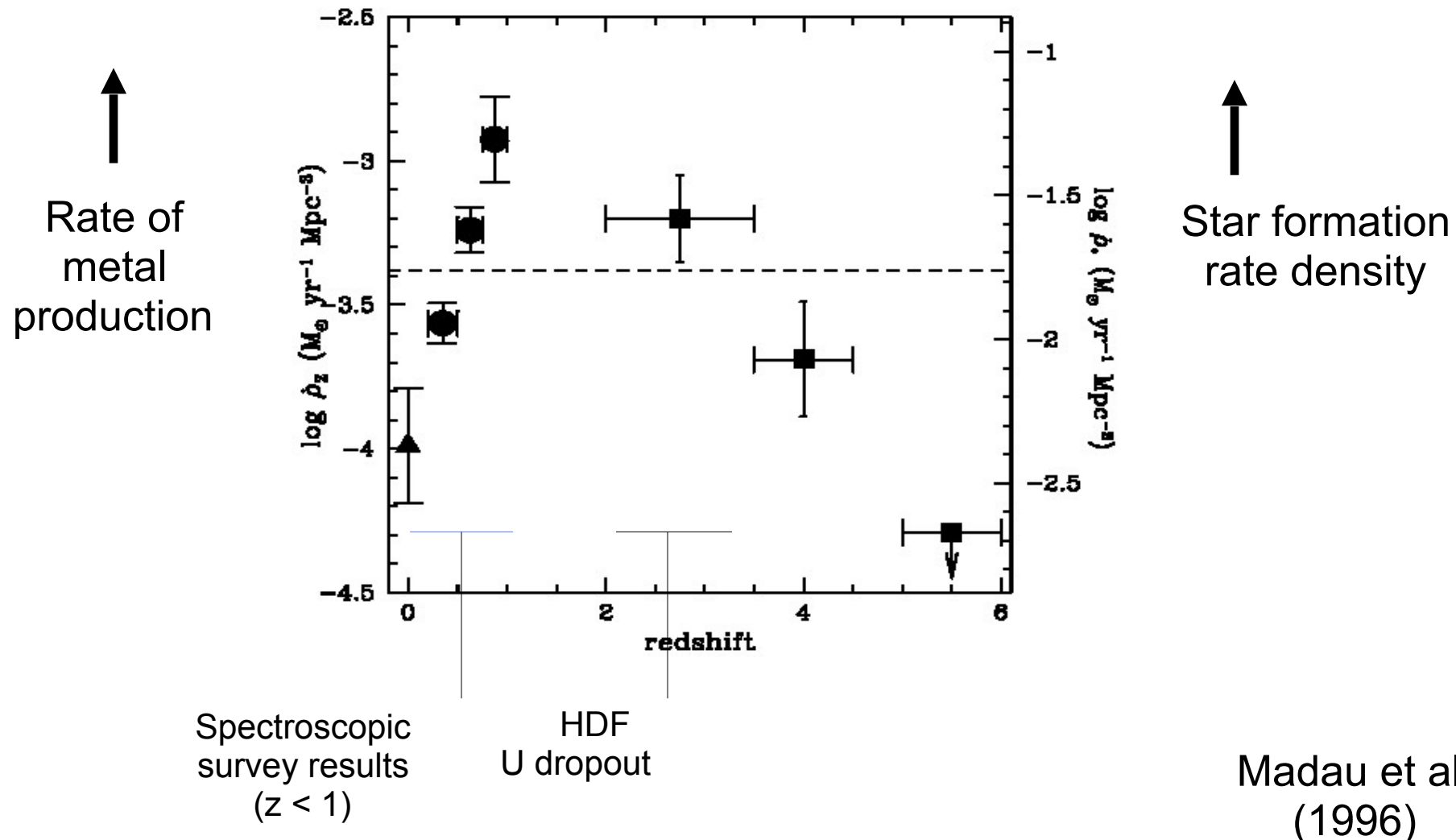


Madau et al.  
(1996)

# The star formation history of the Universe: the “Madau diagram”

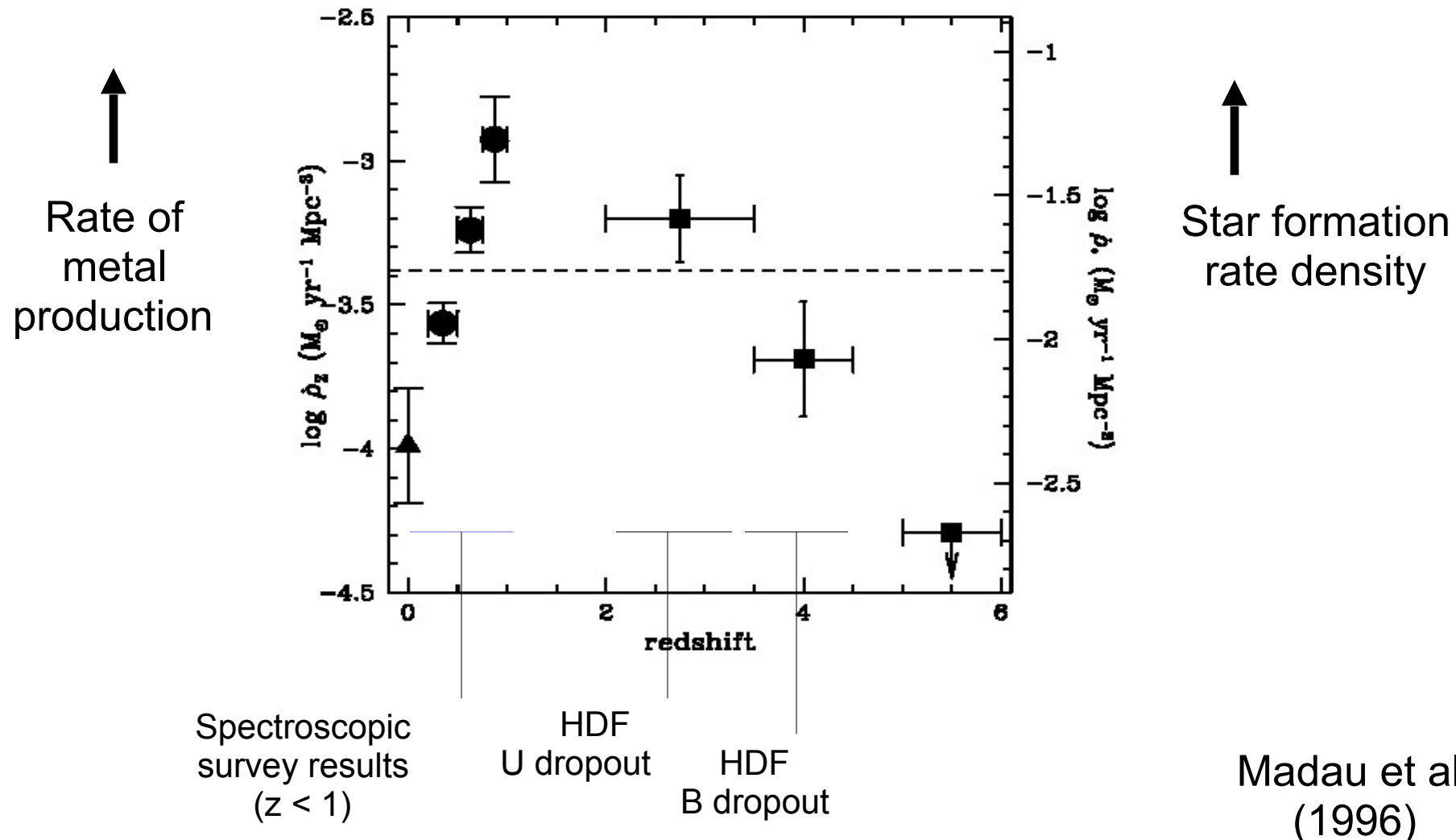


# The star formation history of the Universe: the “Madau diagram”

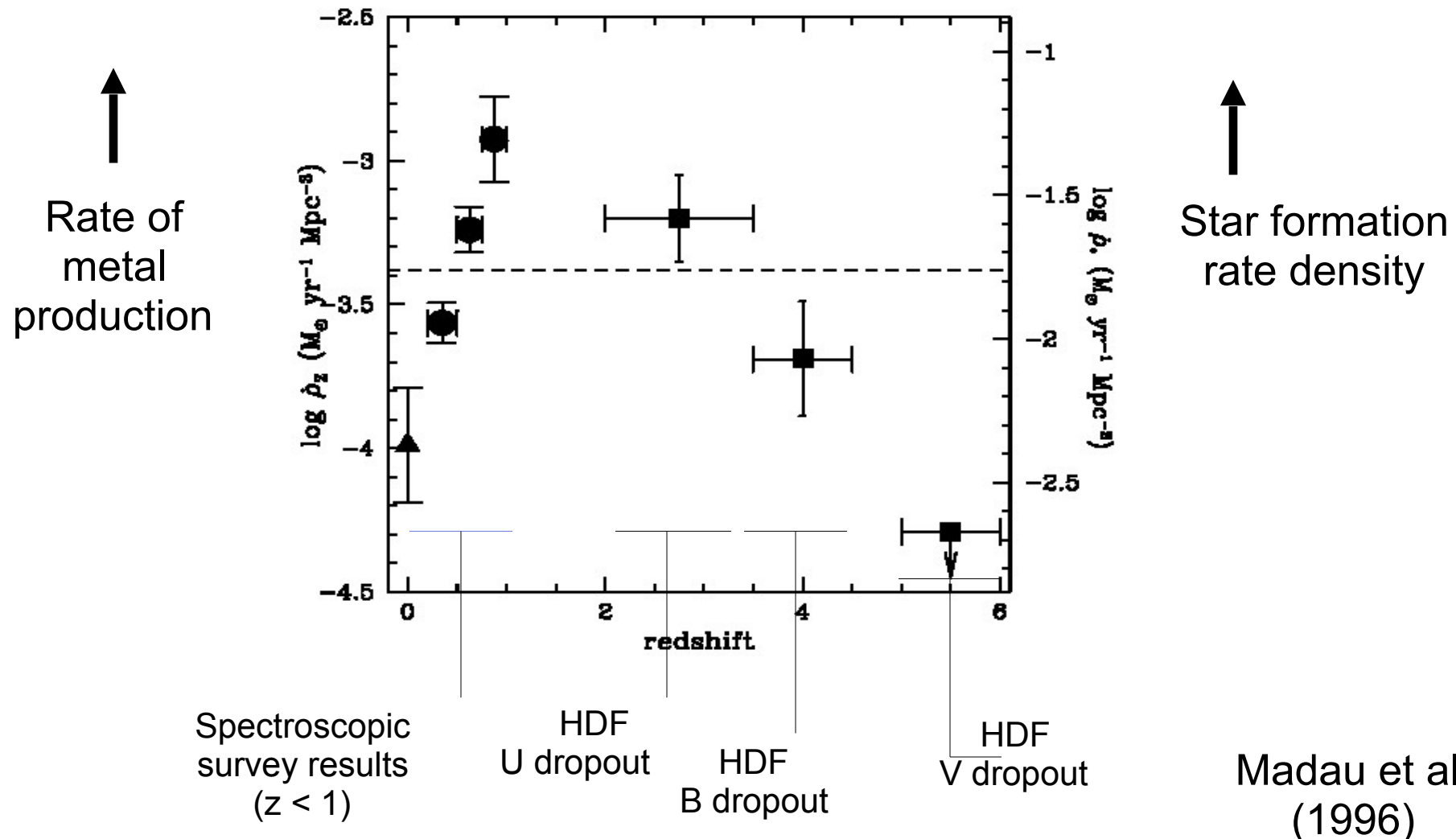


Madau et al.  
(1996)

# The star formation history of the Universe: the “Madau diagram”



# The star formation history of the Universe: the “Madau diagram”



# Madau diagram: summary of preliminary results

- Star formation rate density appears to peak at redshifts  $z \sim 1 - 2$  ( $\sim 6 - 8$  billion years ago)
- The star formation rate density appears to decline by an order of magnitude between  $z=1$  and  $z=0$  and between  $z=2$  and  $z=5$
- The rate of production of metals by hot stars tracks the overall star formation rate (but less uncertain than total SFR because high mass end of the IMF is better defined)
- The peak star formation rate density is:  $\sim 0.1$  solar mass per year per  $\text{Mpc}^{-3}$  (but most of the cosmic volume is empty, and SFR density is much higher than this in galaxies: up to 100s of solar masses per year per  $\text{kpc}^{-3}$  in the extreme case)

# Uncertainties in Madau diagram (all redshifts)

- HST images are sensitive to the high surface brightness peaks in galaxies, but a substantial fraction of the UV light may be in more diffuse structures just below the detection threshold (lost in the noise)
- UV fluxes and luminosities strongly affected by (uncertain) dust extinction
- Conversion from UV luminosity to rate of formation of massive stars depends on understanding of the evolution of massive stars
- Conversion of rate of formation of massive stars to total star formation rate strongly depends on the (uncertain) form of the stellar IMF at low mass end

# Uncertainties in Madau diagram (all redshifts)

- HST images are sensitive to the high surface brightness peaks in galaxies, but a substantial fraction of the UV light may be in more diffuse structures just below the detection threshold (lost in the noise)
- UV fluxes and luminosities strongly affected by (uncertain) dust extinction
- Conversion from UV luminosity to rate of formation of massive stars depends on understanding of the evolution of massive stars
- Conversion of rate of formation of massive stars to total star formation rate strongly depends on the (uncertain) form of the stellar IMF at low mass end

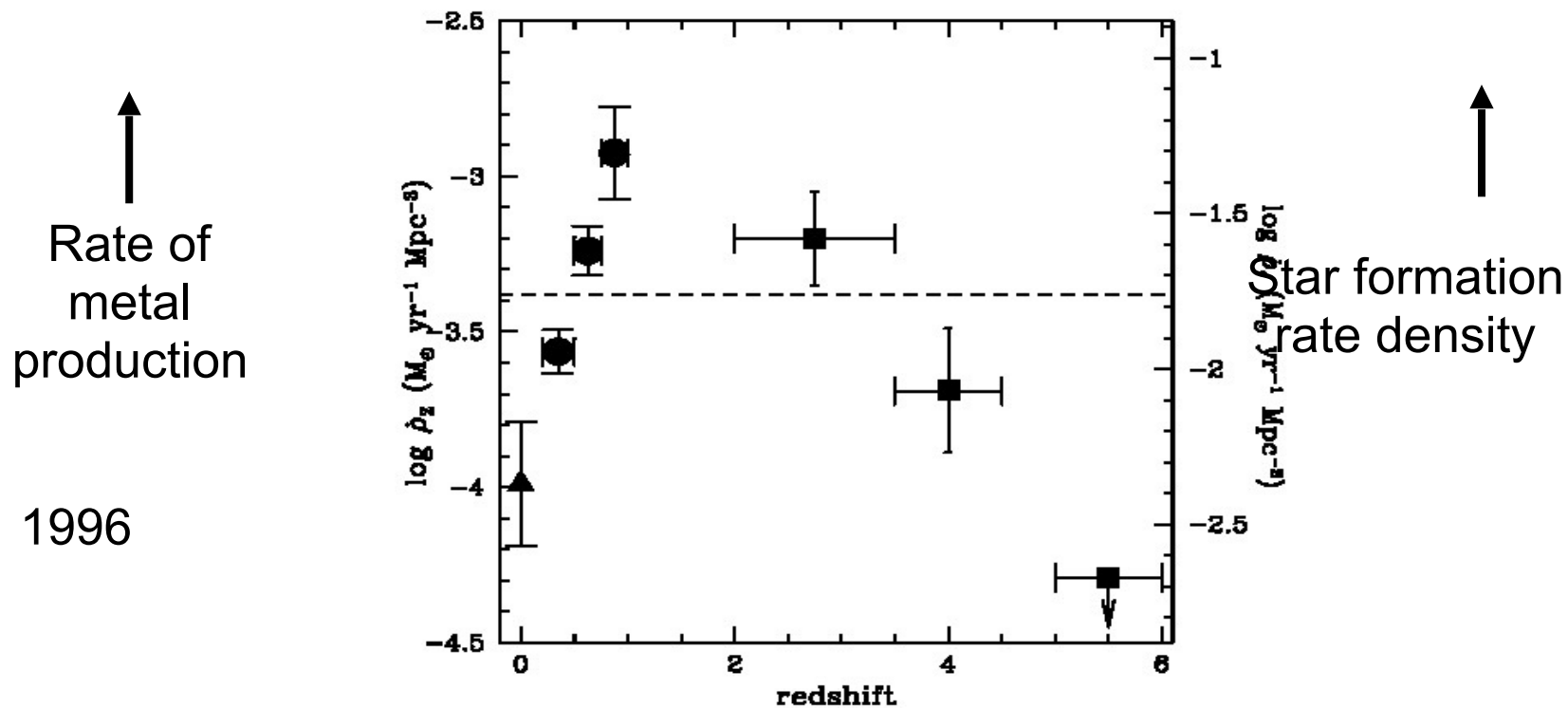
The first two effects above are likely to be the most important, leading to *substantial underestimation* of the SFR density

# The “evolution” of the Madau Diagram

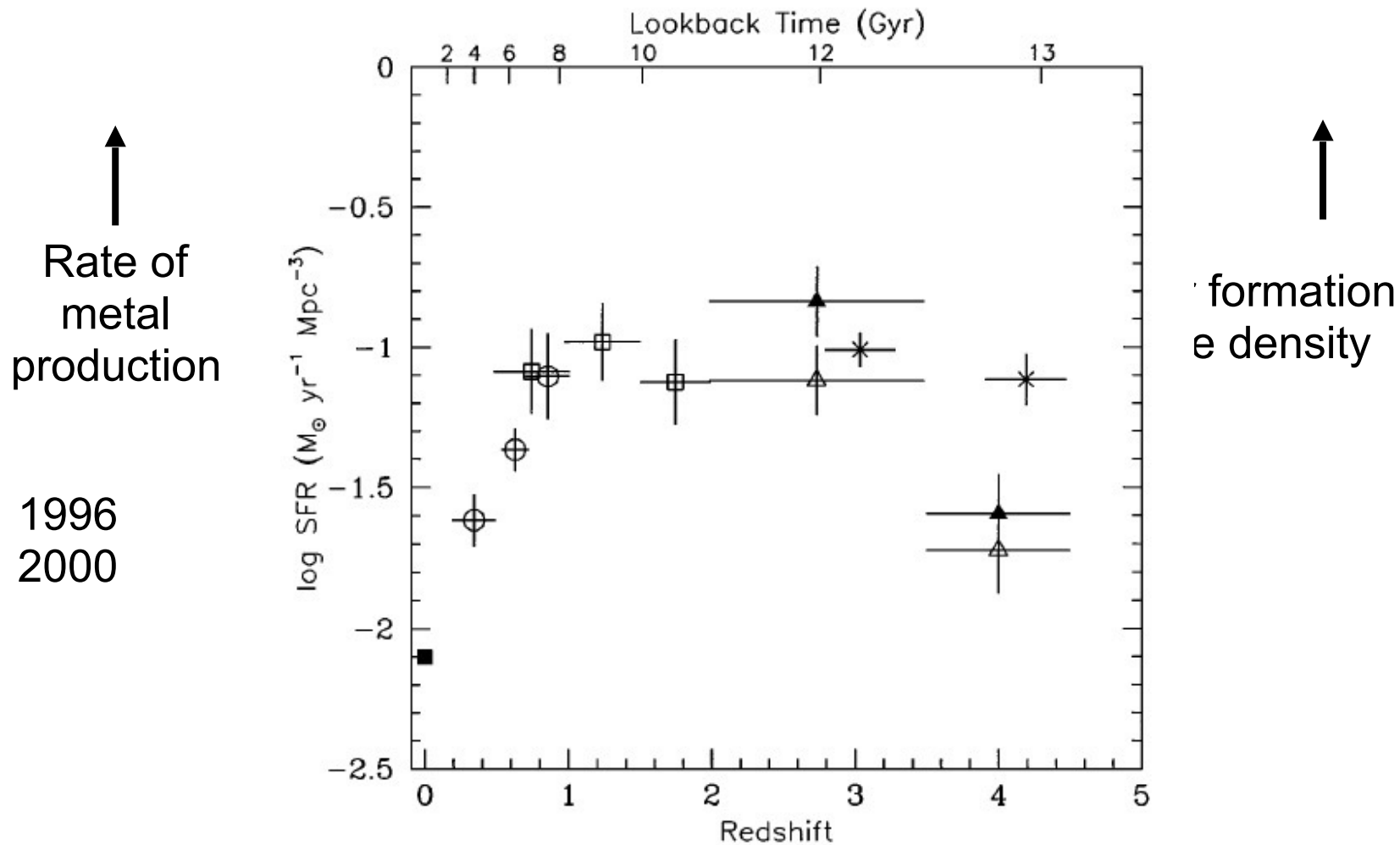
↑  
Rate of  
metal  
production

↑  
Star formation  
rate density

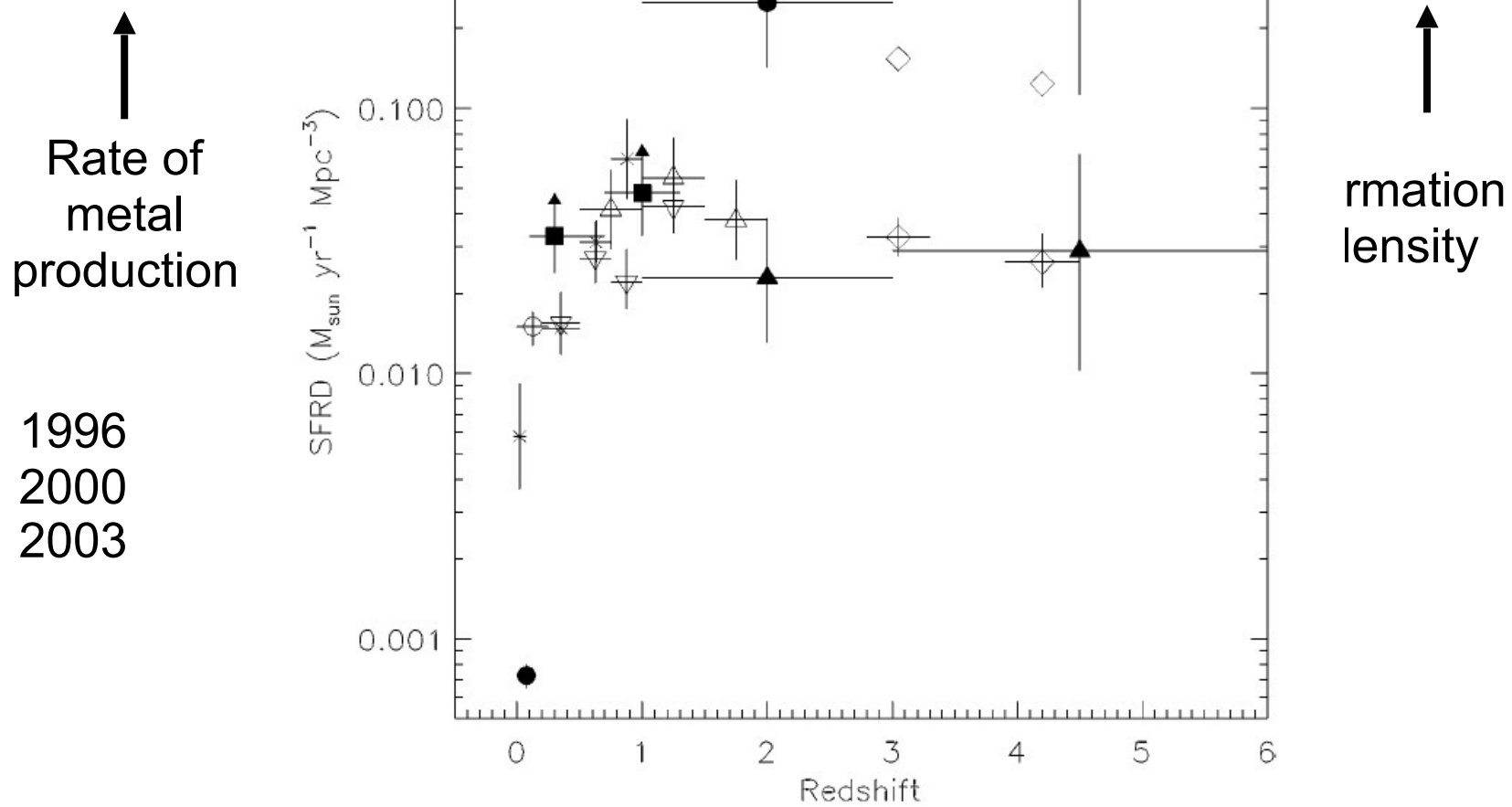
# The “evolution” of the Madau Diagram



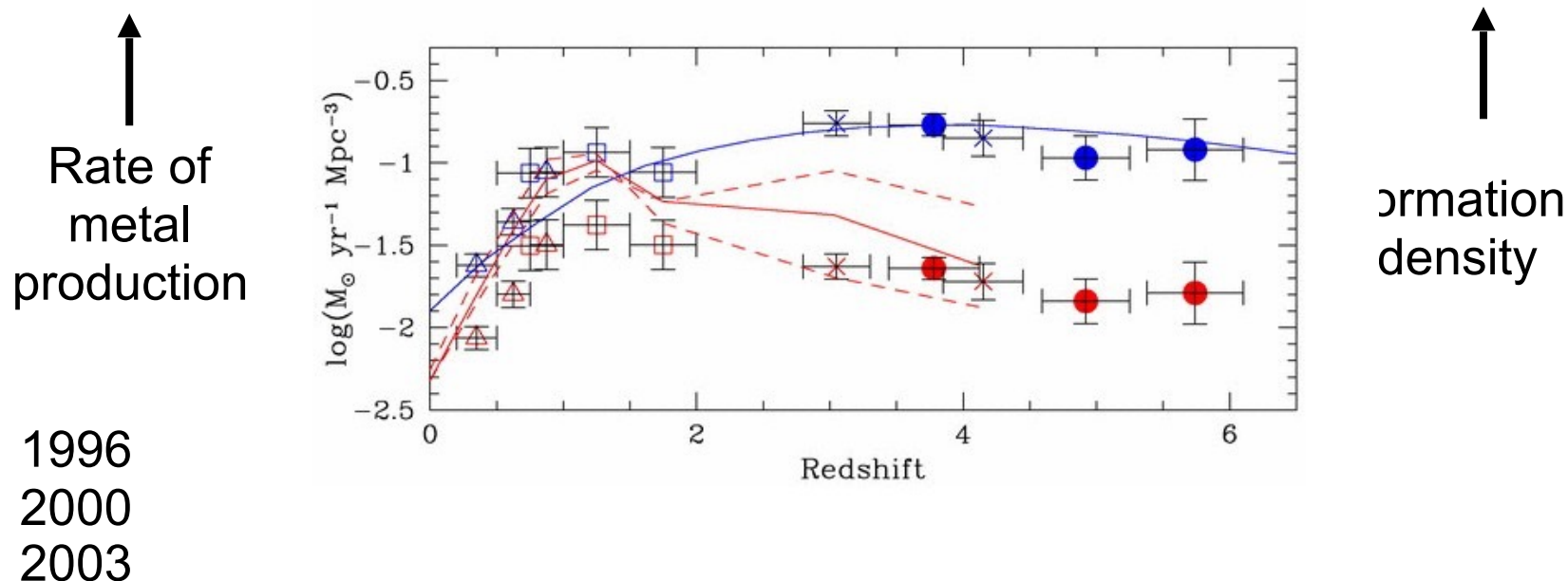
# The “evolution” of the Madau Diagram



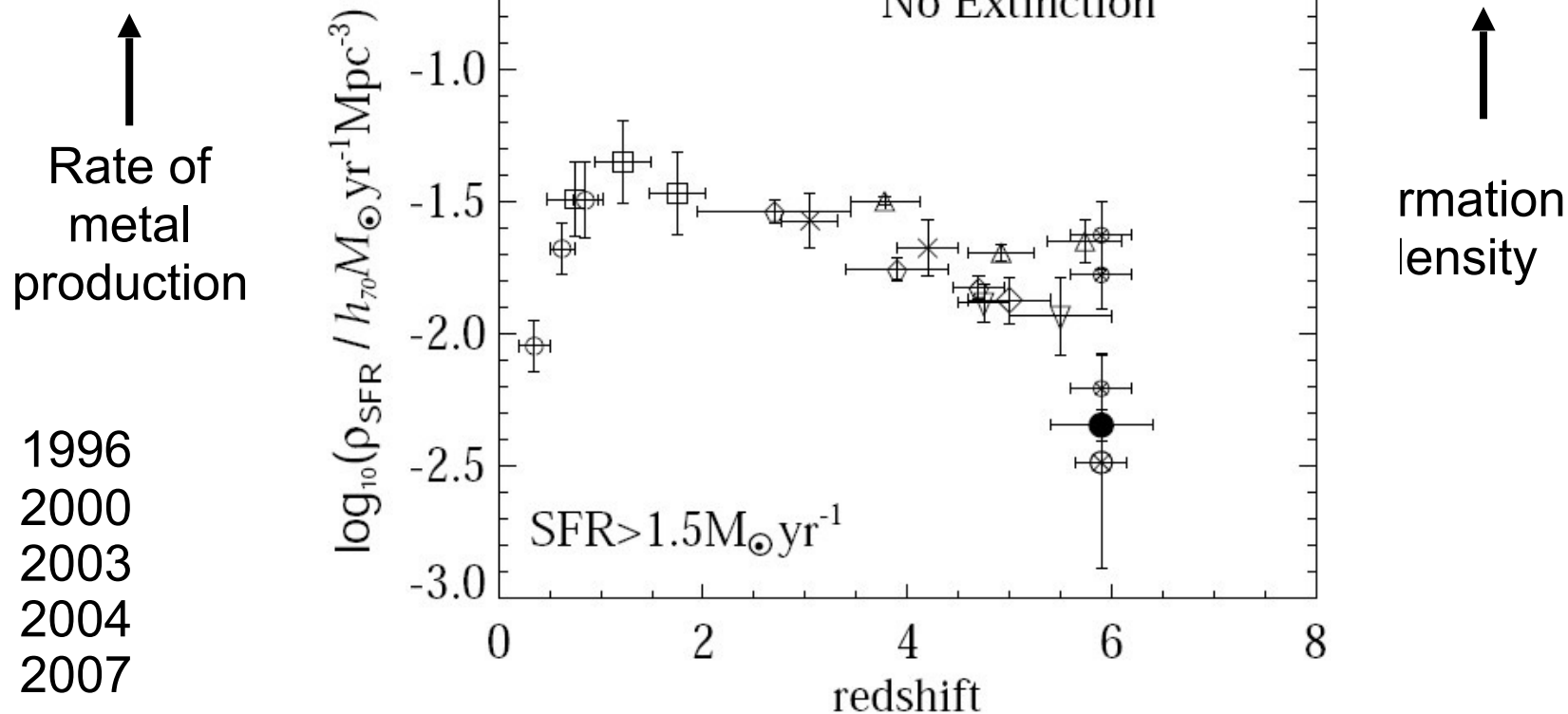
# The “evolution” of the Madau Diagram



# The “evolution” of the Madau Diagram

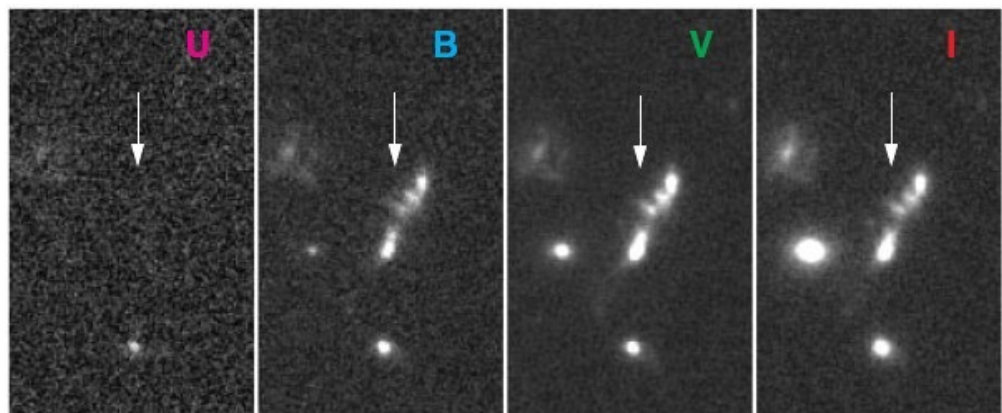
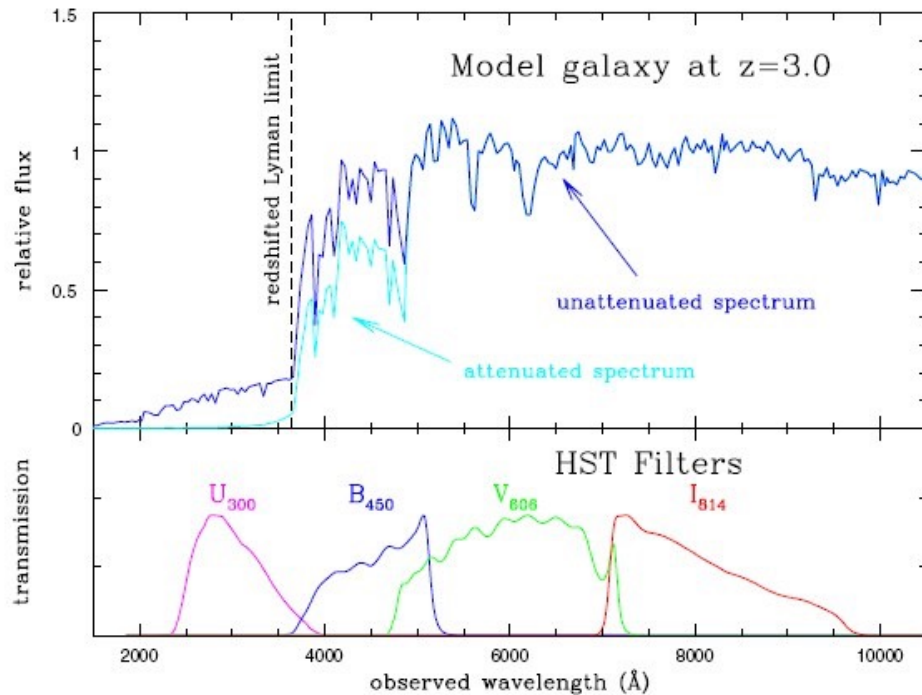


# The “evolution” of the Madau Diagram

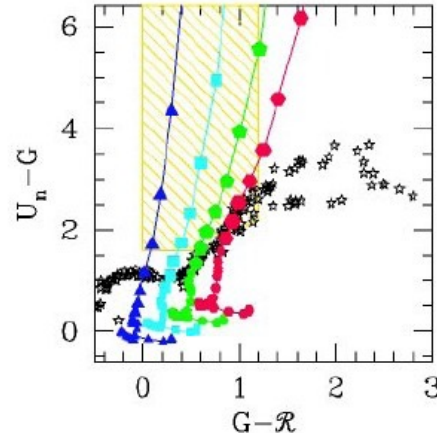
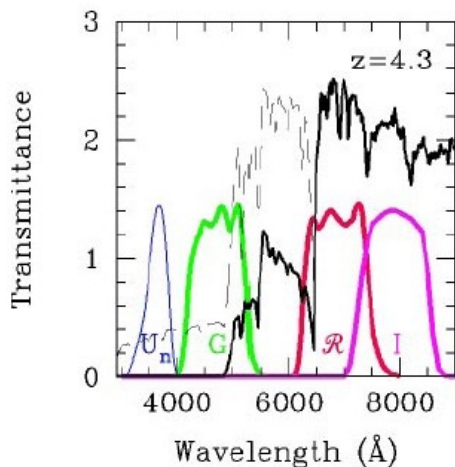
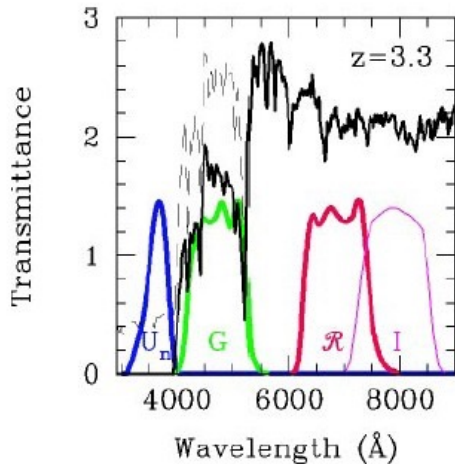


# Redshifts of distant galaxies: example of U-band dropout

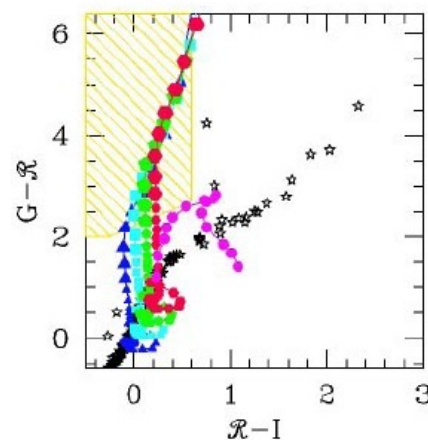
The Lyman dropout technique can be used to detect, and measure redshifts for galaxies that are too faint for conventional spectroscopy.



# Discovery of LBGs



U-band dropouts  
( $2 < z < 3.5$ )



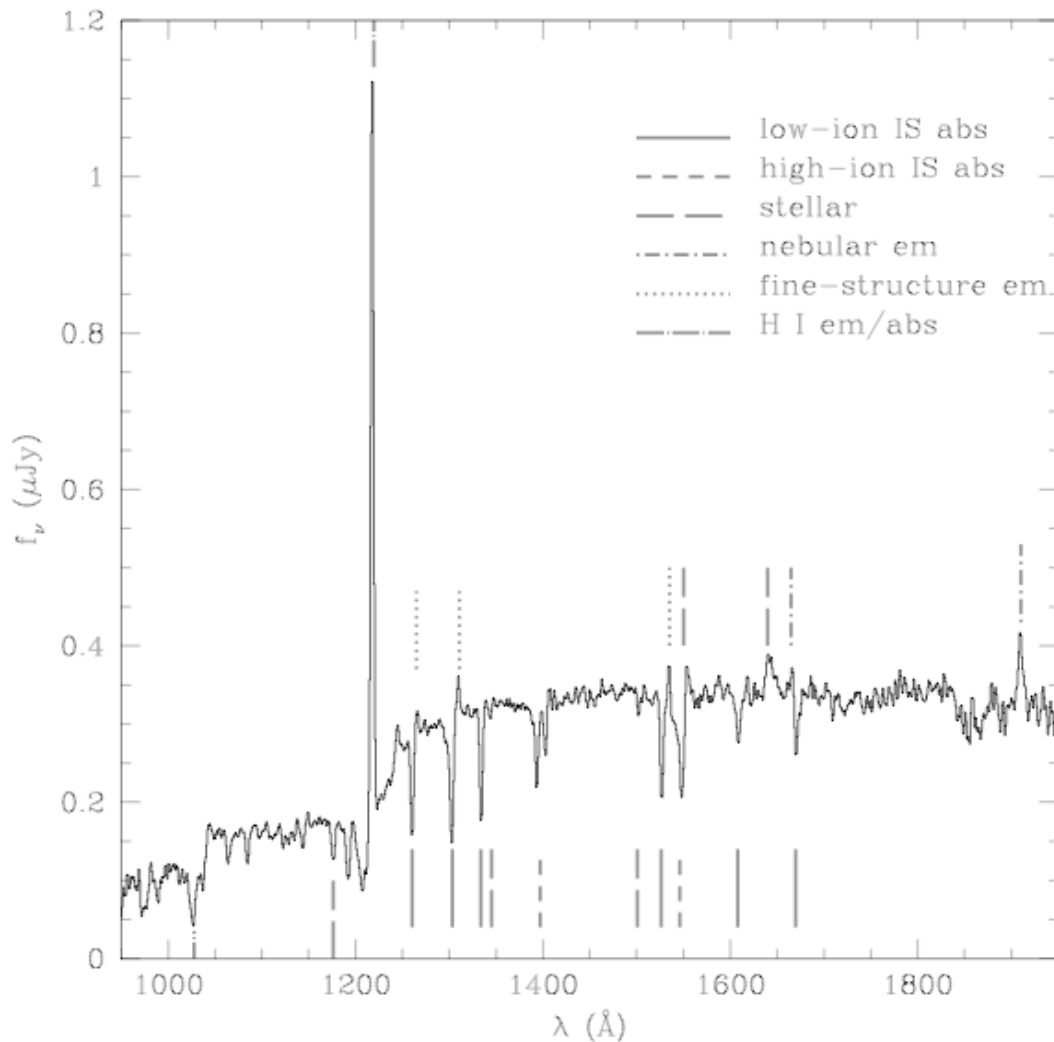
G/B-band dropouts  
( $3.5 < z < 4.5$ )

Lyman dropout technique was first proposed in 1970s (e.g. Meier 1976), but fully developed by Steidel and collaborators in mid-1990s.

# The discovery of Lyman Break Galaxies

- Lyman break galaxies (LBG:  $2 < z < 4.5$ ) are discovered using the Lyman dropout photometric redshift technique with deep imaging observations.
- The brighter candidates are *spectroscopically confirmed* using observations with large (8-10m) telescopes (direct redshifts).
- Although many LBGs ( $\sim 32$ ) have been spectroscopically confirmed in the HDFs, many more ( $> 1000$ ) have been discovered and spectroscopically confirmed in deep ground-based imaging observations of other fields.
- Only the brightest LBGs ( $m_R < 25.5$ ) can be confirmed with spectroscopic observations; the remainder are discovered (but not confirmed) in the HDFs ( $25.5 < m_R < 29.5$ ).

# Average spectrum for (>800!) LBG



LBG spectra show a combination of inter-stellar (IS) emission lines, IS absorption lines, and absorption lines associated with the photospheres of the young stars in the galaxies (the latter tend to be weak!)

# Summary of spectral characteristics of LBGs

- The rest-frame UV spectra of LBGs show narrow absorption lines (e.g. OI, SiII, SiIV, CIV) caused by absorption in the interstellar medium (ISM) of the galaxies.
- Some also show Ly $\alpha$  and CIV emission lines that are also emitted by the galaxies' ISM, but these are generally heavily absorbed, especially in the blue wings, leading to line asymmetries.
- The spectra show marked similarities with the UV spectra of nearby starbursts (e.g. NGC4214).
- Detailed analysis of the fainter absorption lines suggests metal abundances that are sub-solar ( $0.1 < Z_{\text{sun}} < 1$ ), but most of the stronger lines are *saturated*, making accurate abundance determination difficult.

# Morphologies of LBGs

UV Opt.

UV Opt.

UV Opt.



2-454.0  $Z=2.008$



2-449.0  $Z=2.008$



2-585.1  $Z=2.008$



3-118.1  $Z=2.232$



2-903.0  $Z=2.233$



2-525.0  $Z=2.237$



2-82.1  $Z=2.267$



4-445.0  $Z=2.268$



2-824.0  $Z=2.419$



2-239.0  $Z=2.427$



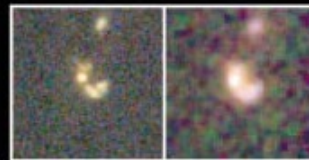
2-591.2  $Z=2.489$



4-639.1  $Z=2.591$



4-555.1  $Z=2.803$



1-54.0  $Z=2.929$



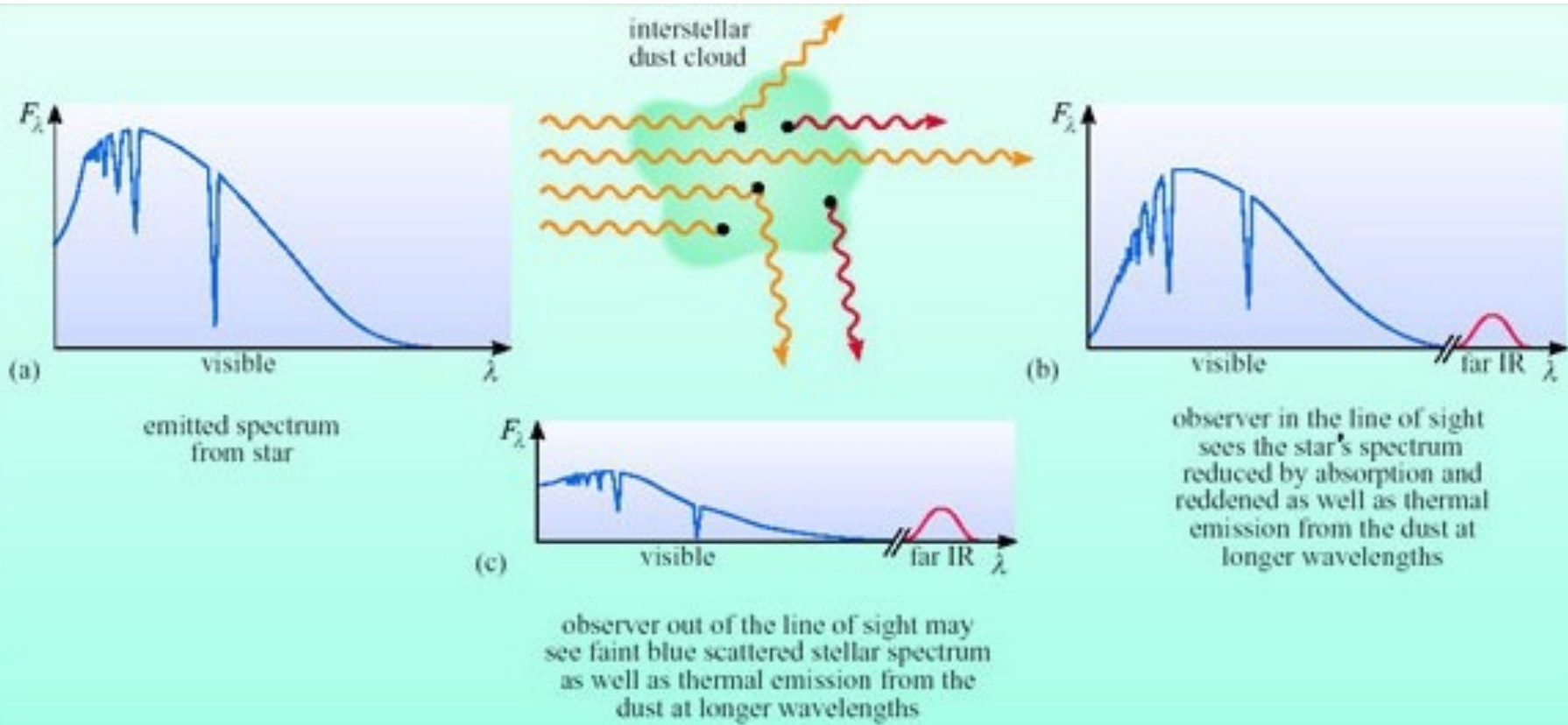
4-52.0  $Z=2.931$

Observations taken with the HST using the WFPC2 camera in the optical (rest frame UV) and the NICMOS camera in the near-IR (rest frame optical).

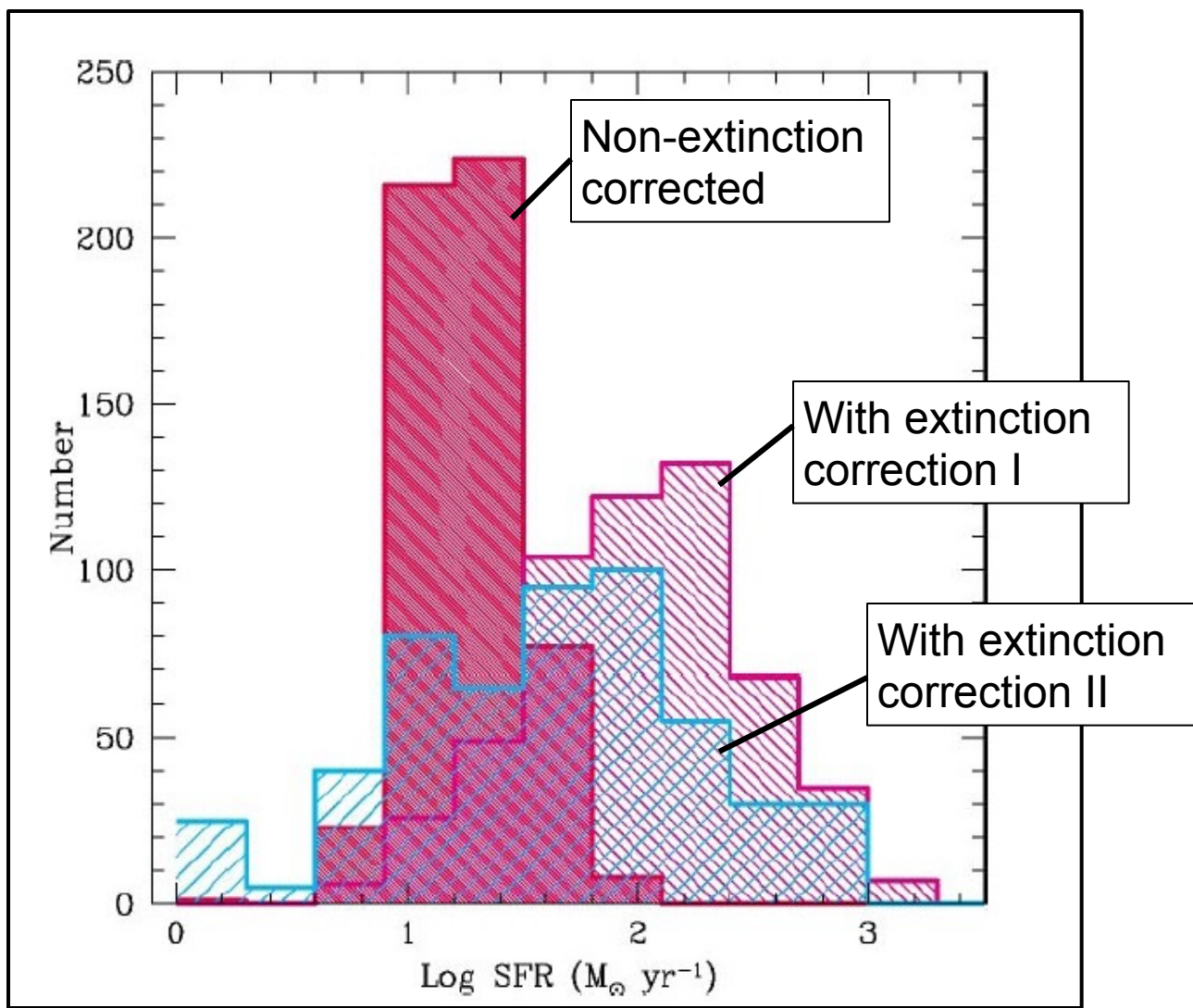
# Summary of LBG morphological properties

- Overall, LBG appear smaller than galaxies of similar luminosity in the local Universe, but their half-light radii (~4 - 7 kpc) are typical of galaxy bulges and low/moderate luminosity ellipticals.
- There is little evidence for a morphological K-correction: LBG appear similar at rest-frame optical and UV wavelengths in high resolution HST images
- A wide range of morphologies is observed, from relatively smooth disk/spheroids to highly clumpy irregular systems.
- But many LBGs show the highly asymmetric or disturbed morphologies that characterise mergers and galaxy interactions in the local Universe.

# Interstellar extinction/reddening - I



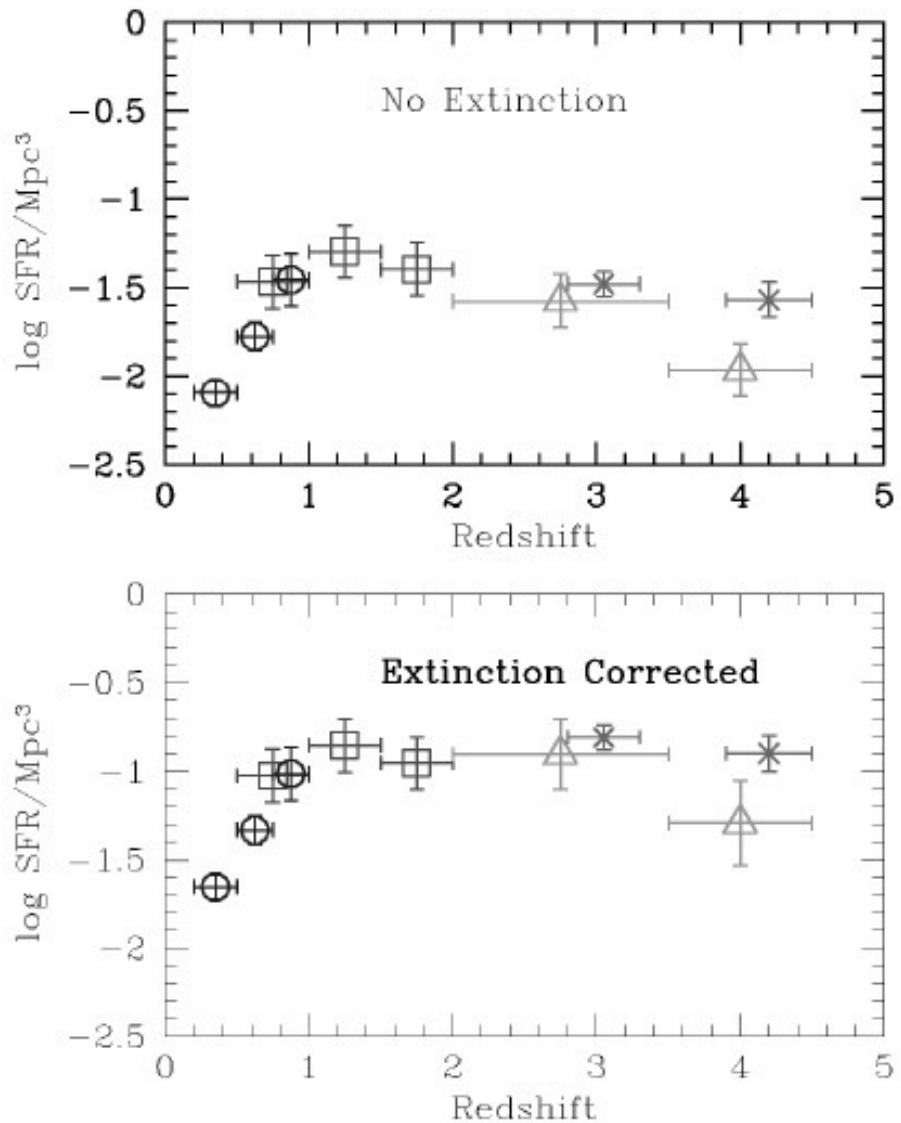
# Statistics of star formation rates for LBG



# Madau diagram revisited

Triangles: HDF results  
Stars: LBG results (ground-based detections)

Note: Because of their larger numbers, the LBG detected in ground-based observations give better statistics (smaller error bars) than the much smaller sample detected in the HDF.



# Star formation history of the Universe from observations of LBGs

- The slopes/colours of the UV continua are characteristic of lightly reddened starburst spectra with  $0.1 < E(B-V) < 0.45$ .
- Correcting for the reddening boosts the luminosities and implied star formation rates by a factor  $\sim 3\text{-}10x$ .
- The extinction-corrected star formation rates ( $\sim 10 - 1000 M_{\text{sun}} \text{ yr}^{-1}$ ) are characteristic of extreme starbursts in the local Universe, but the UV light is more spatially diffuse than the most extreme local starbursts (e.g. ULIRGs).
- The extinction correction boosts the global SFR rate in Madau diagram at high redshifts, removing the apparent peak at  $z\sim 1\text{-}2$ ; the SFR now appears to remain roughly constant at  $z > 2$ .

# Volume density of LBGs

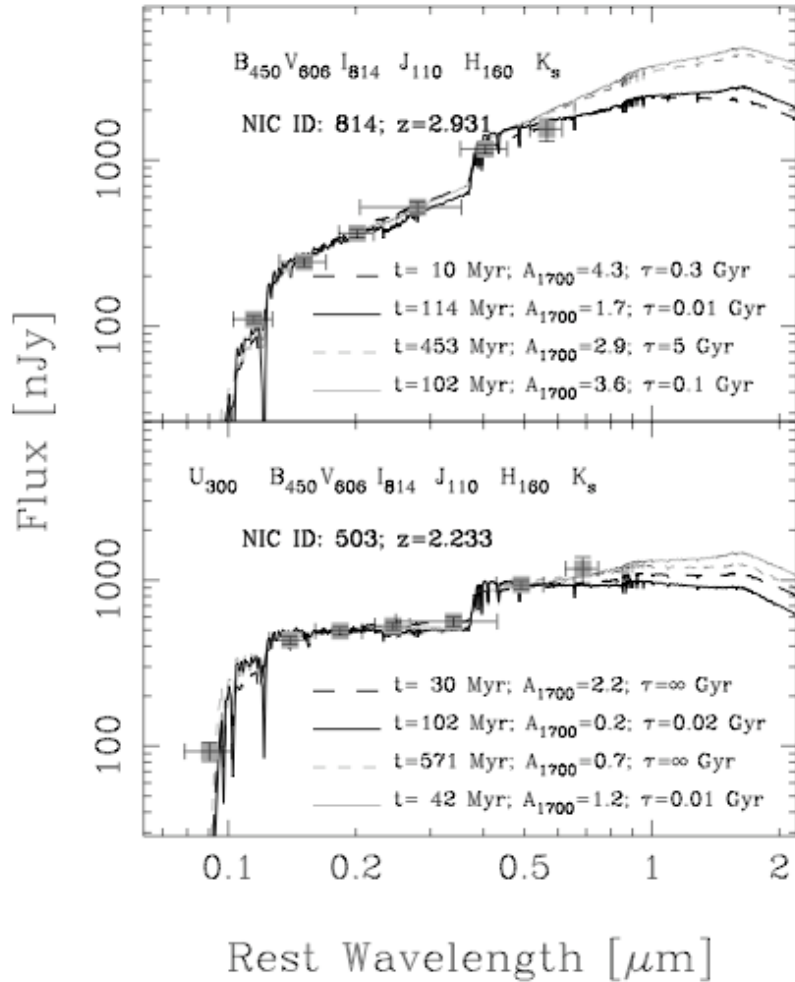
- The luminosity function for LBGs can be fitted with a Schechter function.
- The volume density of LBGs at the break of the luminosity function is similar to that of  $L^*$  galaxies in local Universe.
- There is no evidence for any evolution in the luminosity function of LBGs between  $z \sim 4$  and  $z \sim 3$ .
- Surface density of LBGs:

$$\Sigma_U(25.5) = 1.21 \pm 0.06 \text{ galaxies arcmin}^{-2}$$

$$\Sigma_G(25.5) = 0.47 \pm 0.02 \text{ galaxies arcmin}^{-2}$$

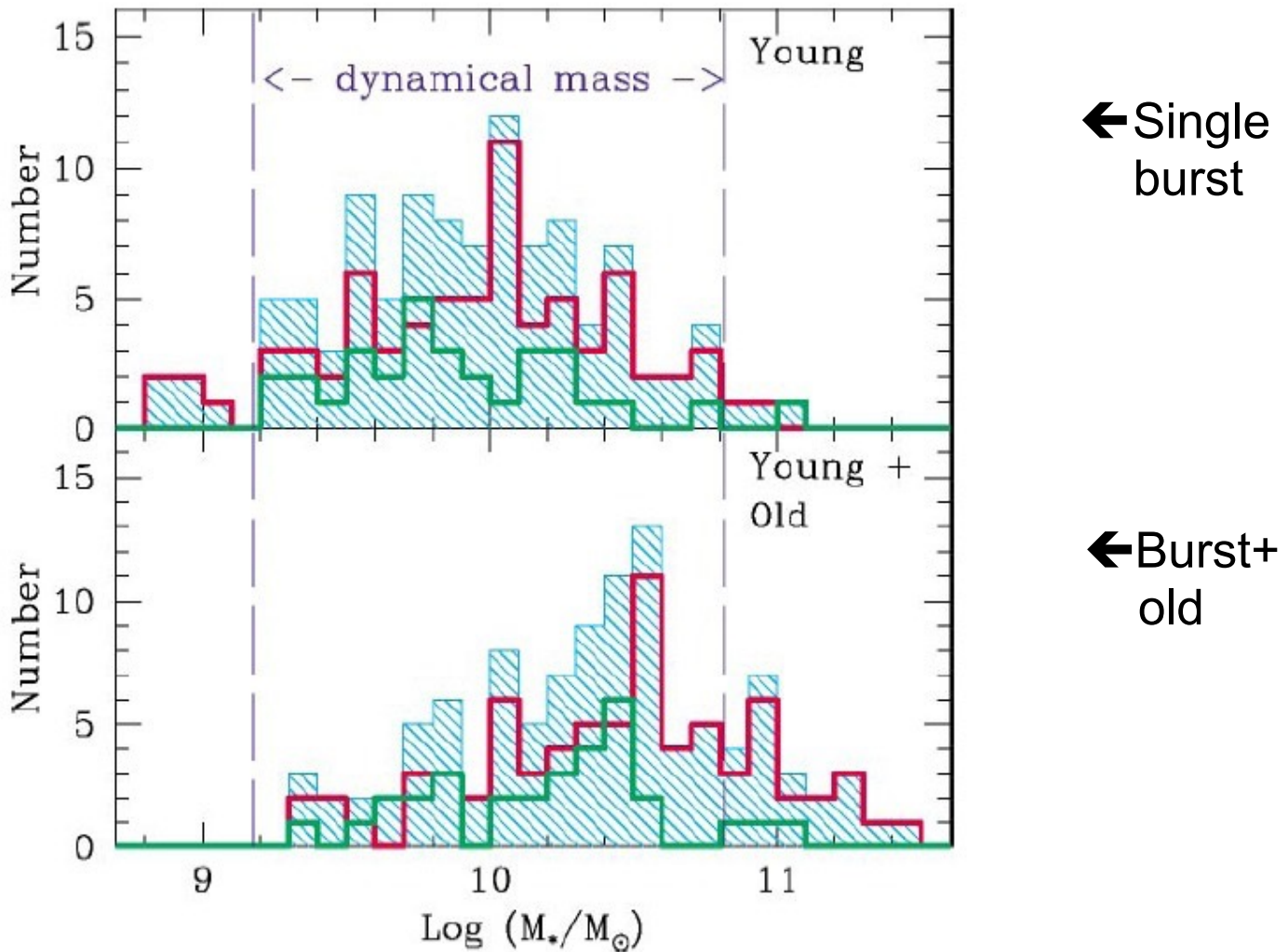
for U and G (B) dropouts down to 25.5 and 25 magnitudes respectively.

# Masses of LBGs I: Spectral synthesis models

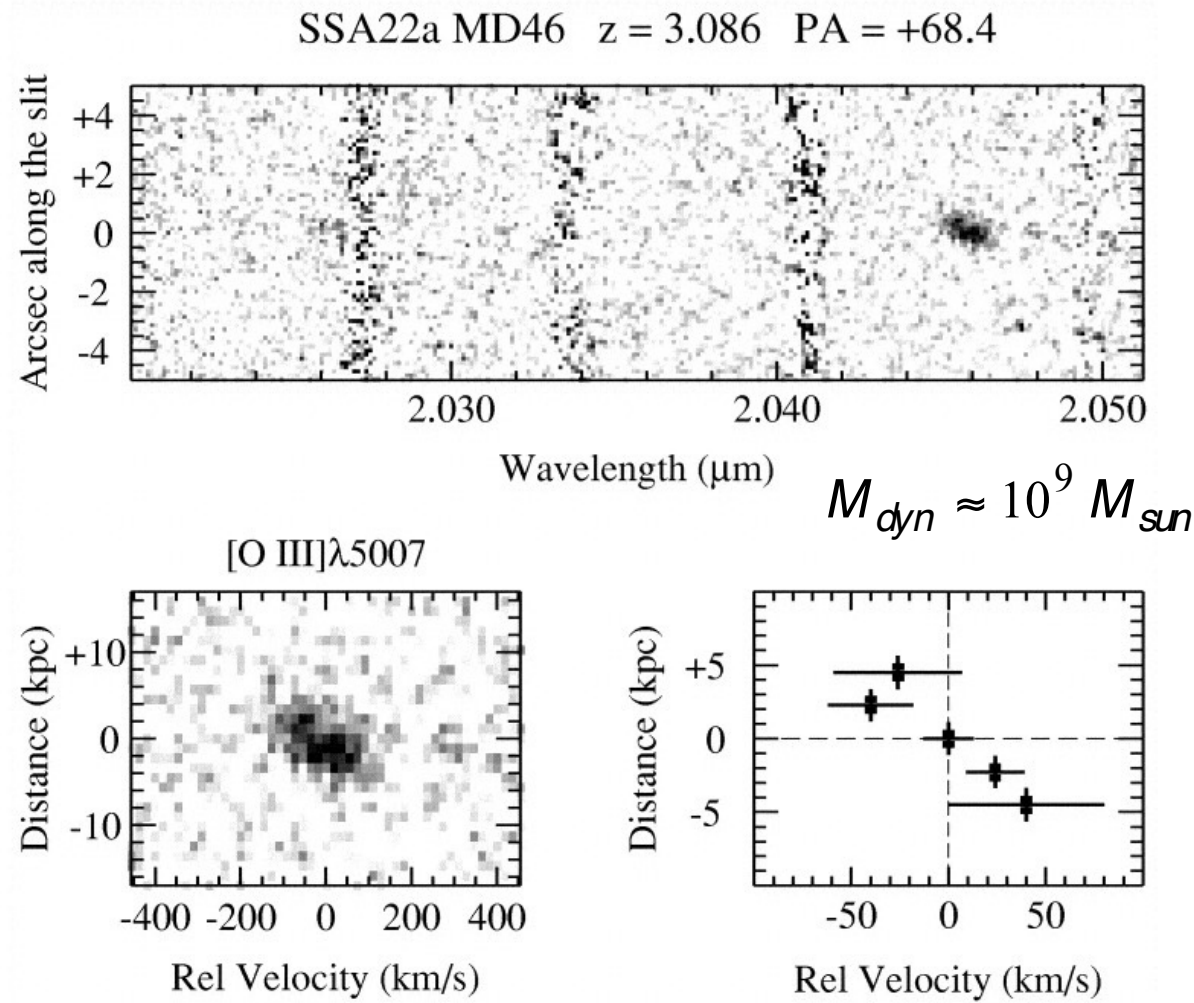


Fit spectral synthesis models of various age, reddening, metallicity to broad-band photometric fluxes (B,V,I,J,H,K) determined from deep optical and near-IR HST images

# Masses of LBGs I: Stellar mass distribution and range



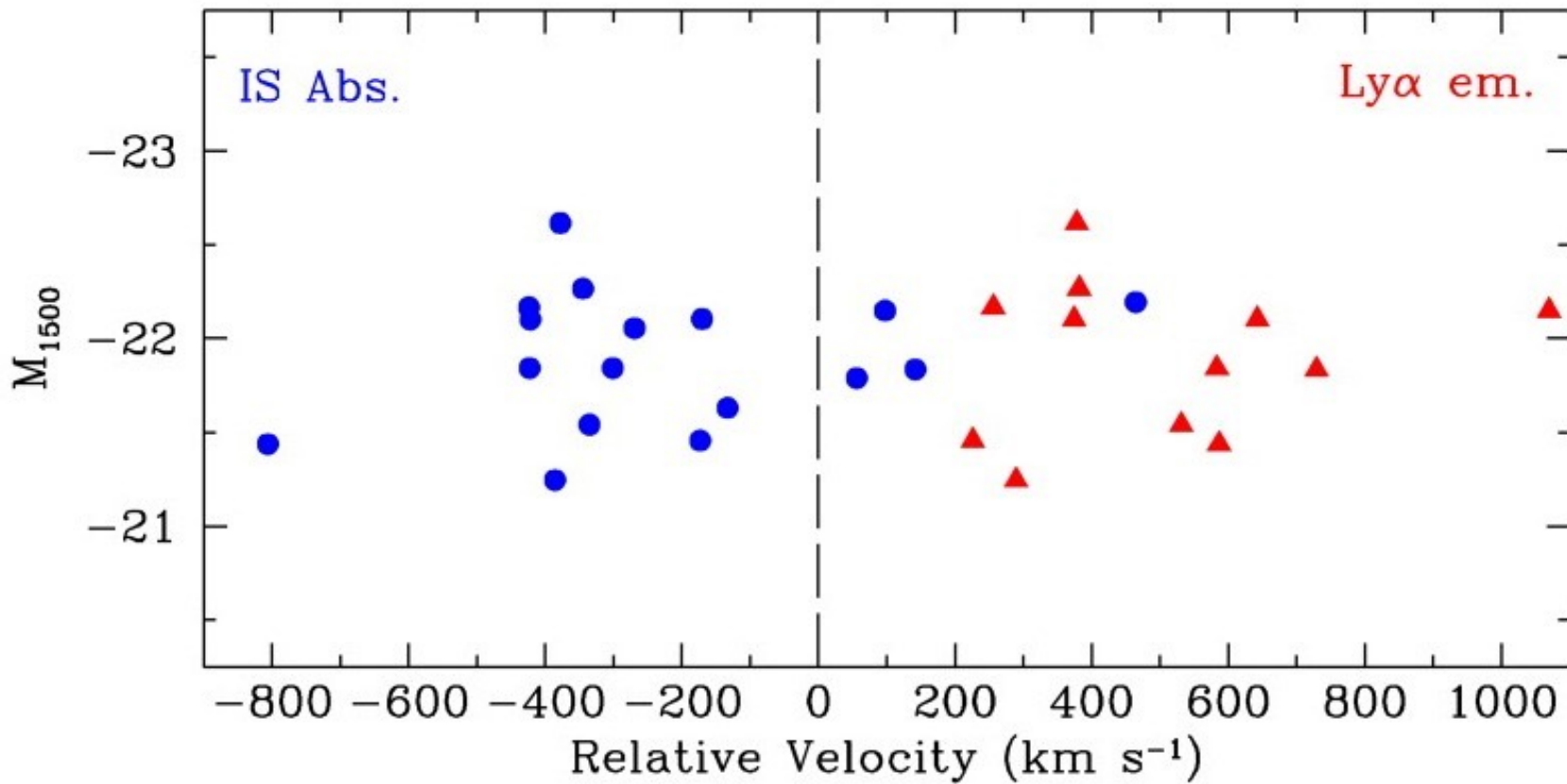
# Masses of LBGs II. Dynamical masses from rotation curves



# Summary of LBG mass estimates

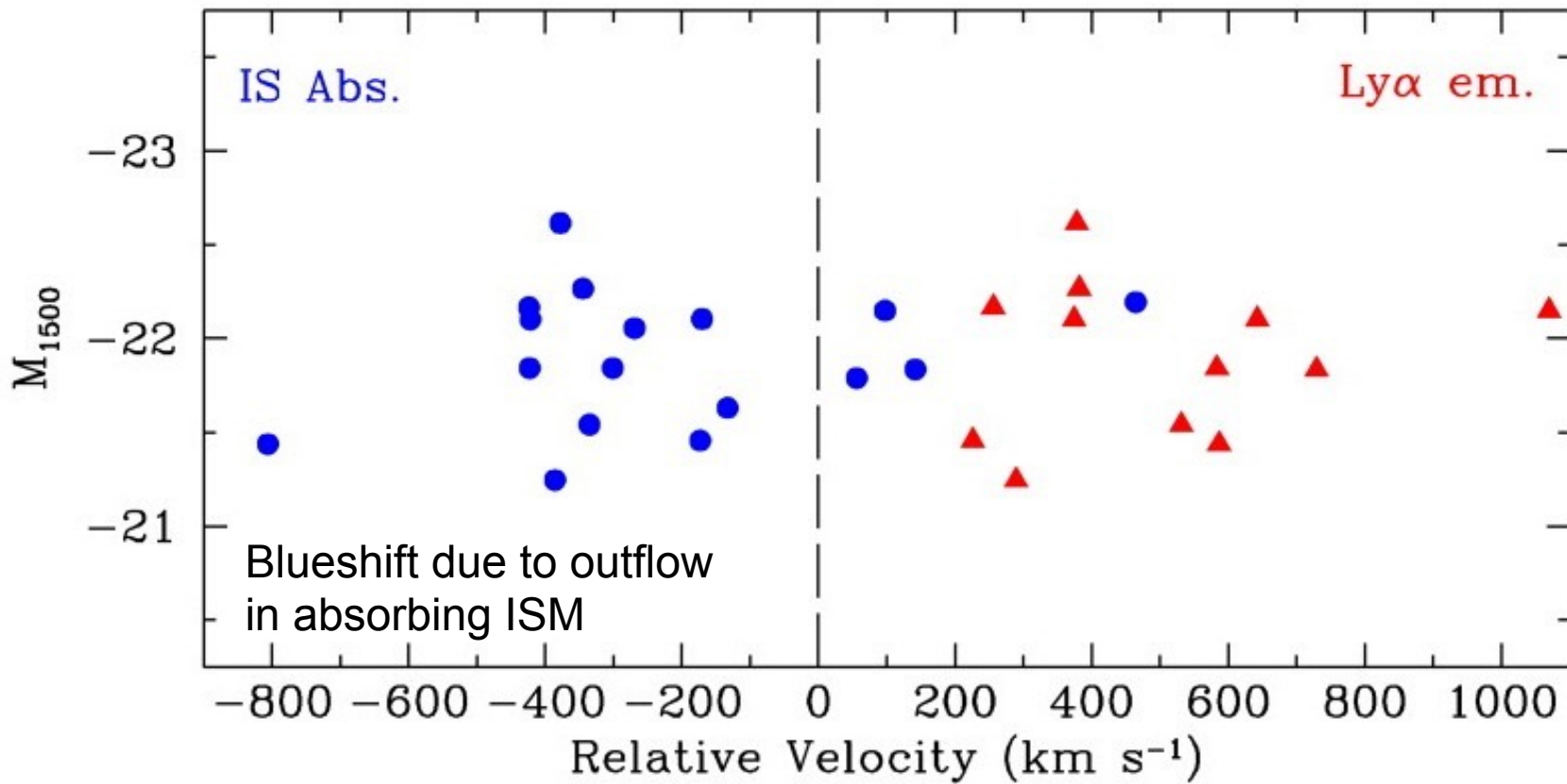
- Spectral synthesis modelling of the broad-band spectral energy distributions of the LBGs yields *stellar* masses:  $10^{10} - 10^{11} M_{\text{sun}}$ .
- The dynamical modelling estimates of the *total* masses of LBGs cover a similar range or lower:  $10^9 - 10^{11} M_{\text{sun}}$ .
- For comparison, a typical  $L^*$  galaxy in the local universe (e.g. Milky Way) has a stellar mass of  $M_{\text{star}} \sim 10^{11} M_{\text{sun}}$  and a total mass of  $10^{12} M_{\text{sun}}$  (the total mass includes dark matter).
- This suggests that the dynamical masses of LBGs may be substantially underestimated.

# Evidence for outflows in LBGs



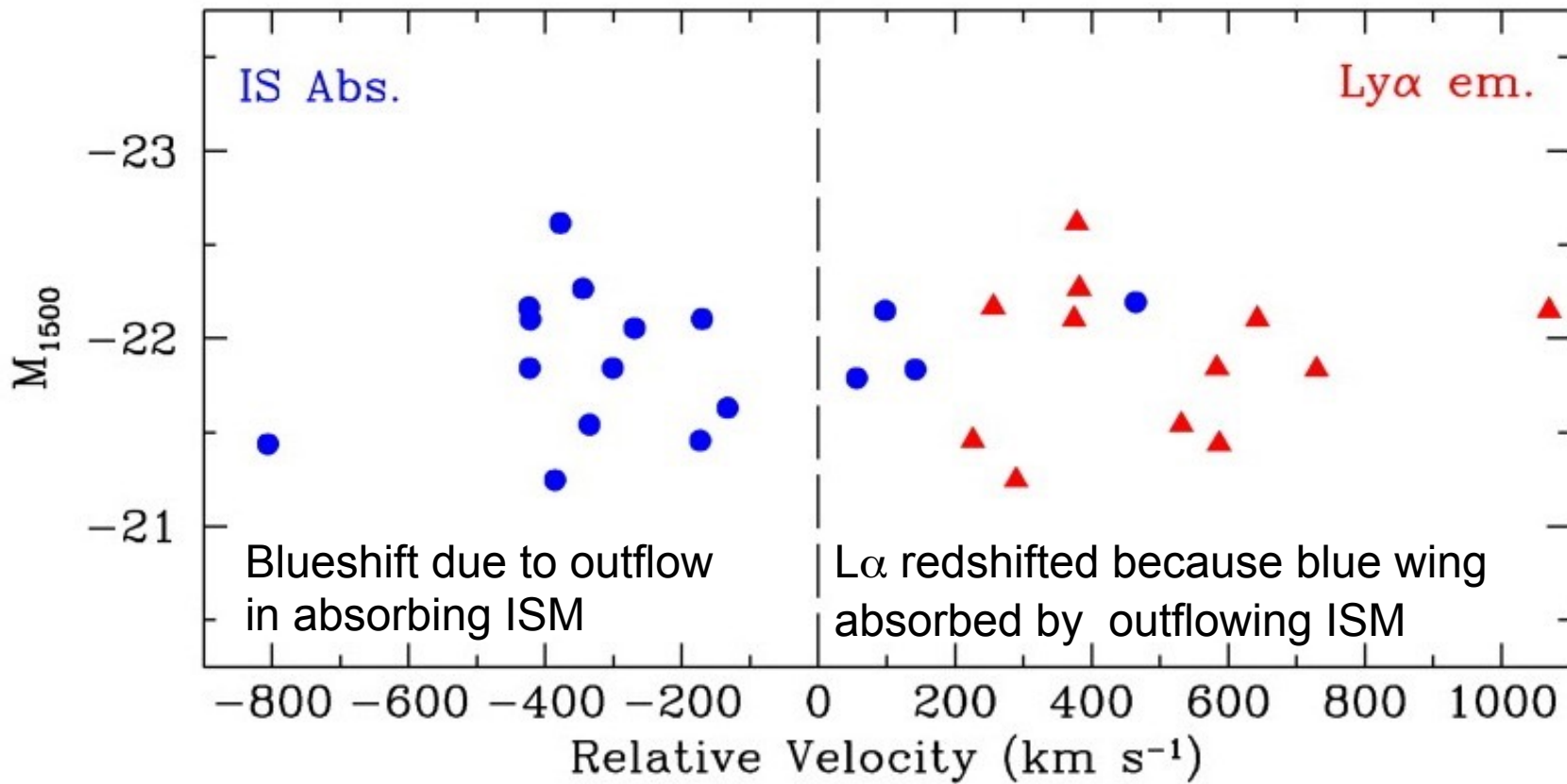
Shift of ISM absorption lines and Ly $\alpha$  emission line  
relative to rest frame defined by optical emission lines  
observed in near-IR (Pettini et al. 2001).

# Evidence for outflows in LBGs



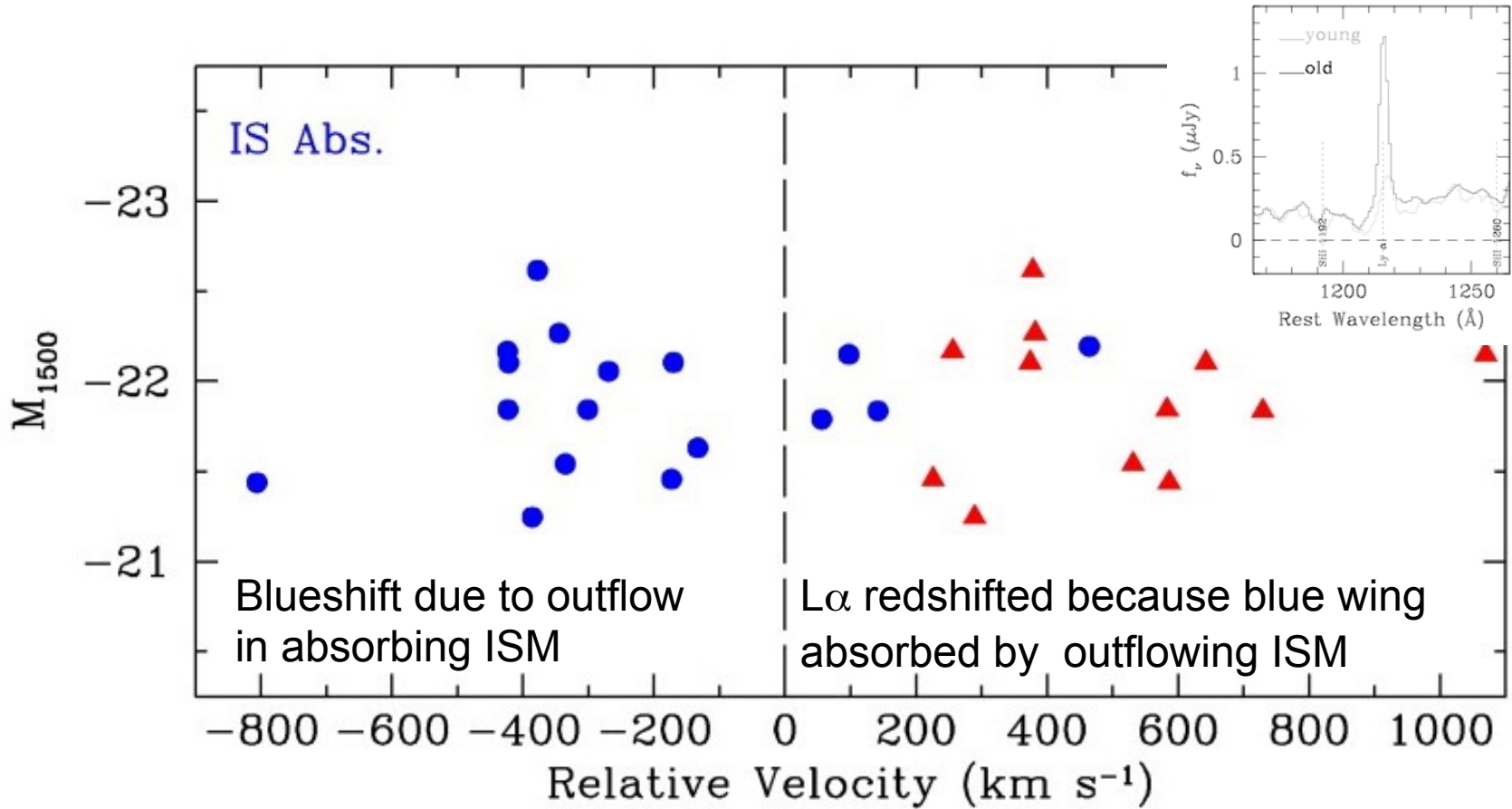
Shift of ISM absorption lines and  $\text{Ly}\alpha$  emission line relative to rest frame defined by optical emission lines observed in near-IR (Pettini et al. 2001).

# Evidence for outflows in LBGs



Shift of ISM absorption lines and Ly $\alpha$  emission line relative to rest frame defined by optical emission lines observed in near-IR (Pettini et al. 2001).

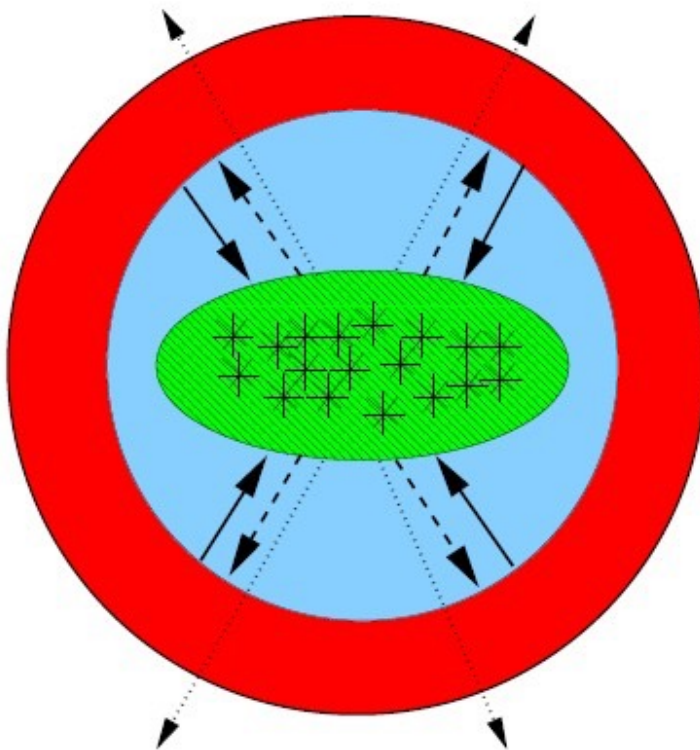
# Evidence for outflows in LBGs



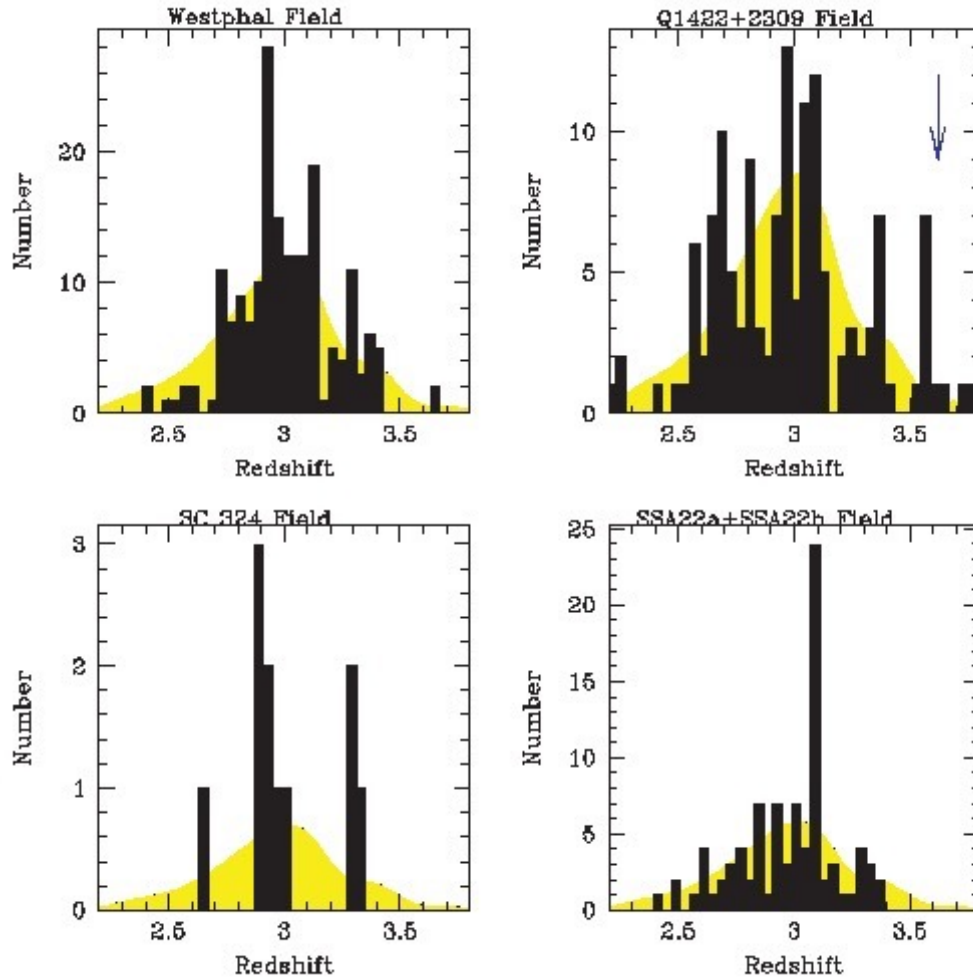
Shift of ISM absorption lines and Ly $\alpha$  emission line relative to rest frame defined by optical emission lines observed in near-IR (Pettini et al. 2001).

# Outflows in LBG

- The emission line and absorption line kinematics measured in LBG suggest that they are driving mass outflows (superwinds).
- Such outflows -- thought to be associated with the accumulated SN explosions of massive stars in starbursts -- are an important ingredient of the semi-analytic galaxy formation models.

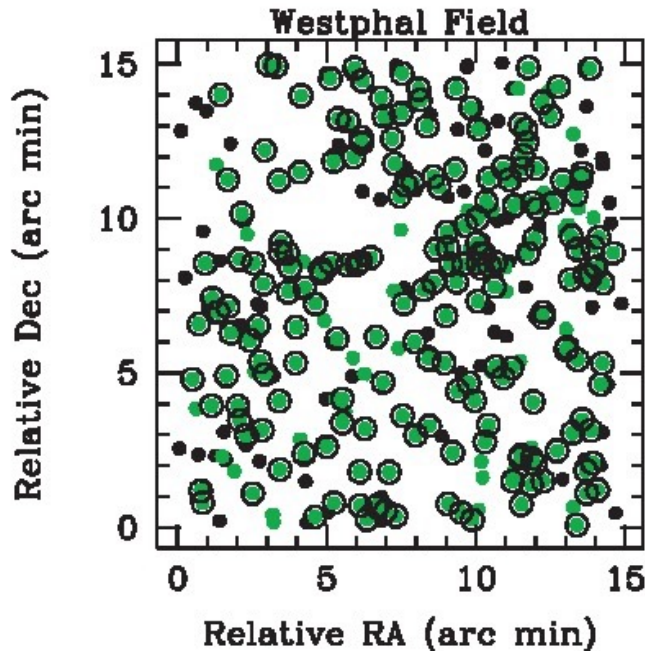


# Clustering of LBGs: Clustering in redshift



The LBG redshift distributions in various fields show strong, narrow peaks at certain redshifts that are significantly above the expected redshift distribution (yellow: based on the average redshift distribution of all the LBGs in the fields observed in the ground-based studies).

# Clustering of LBGs II. Angular and spatial clustering



The correlation length found for LBG  $r_0 \sim 6\text{-}9$  Mpc, is similar to that found for local galaxies ( $r_0 \sim 8$  Mpc), suggesting a similar degree of galaxy clustering.

The clustering of LBGs can be quantified using the two point angular correlation function:

$$N(\theta)d\Omega = n_g[1 + w(\theta)]d\Omega$$

This can be converted to the two point spatial clustering function:

$$N(r)dV = N_g[1 + \xi(r)]dV;$$

$$\xi(r) = \left(\frac{r}{r_0}\right)^{-\gamma}$$

# Lyman break galaxies: where are they now?

- By the current epoch the stellar populations we observe forming in the LBGs at high redshifts would appear old ( $\sim$ 10 billion years).
  - The characteristic radii and stellar masses of the LBGs are similar to those of galaxy bulges and low/moderate luminosity elliptical galaxies in the local Universe.
  - But the morphologies of LBGs are generally more disturbed than local galaxies.
- *The properties of LBGs are consistent with them being nascent galaxy bulges and low/moderate luminosity elliptical galaxies forming hierarchically by galaxy mergers in the early Universe.*

# Lecture7: learning outcomes

- Detailed knowledge of the history of discovery of LBG galaxies using Lyman dropout techniques
- An appreciation of the importance of correcting for dust extinction/reddening when calculating star formation rates
- Knowledge of the general properties of LBGs (radii, reddening, masses, abundances, star formation rates), and how they were derived
- An understanding of possible links between LBG and galaxies in the local Universe (where are they now?)

on

increase  
pattern is a  
due to the fact  
that WFPC2  
has 4 CCDs  
that take  
images  
simultaneously

Williams et al.  
(1996)



Hubble Deep Field

ST Scl OPO January 15, 1996 R. Williams and the HDF Team (ST Scl) and NASA

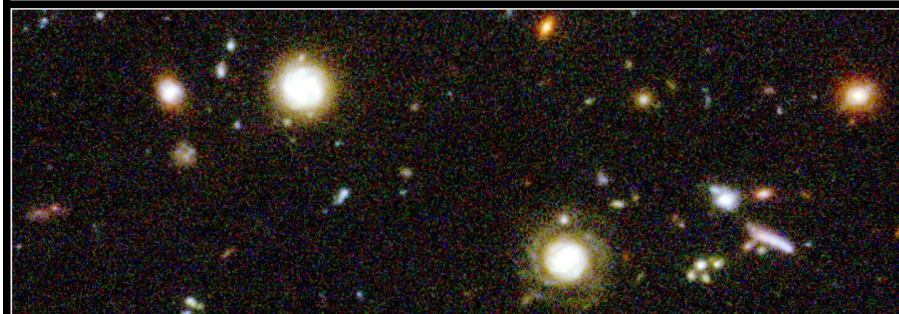
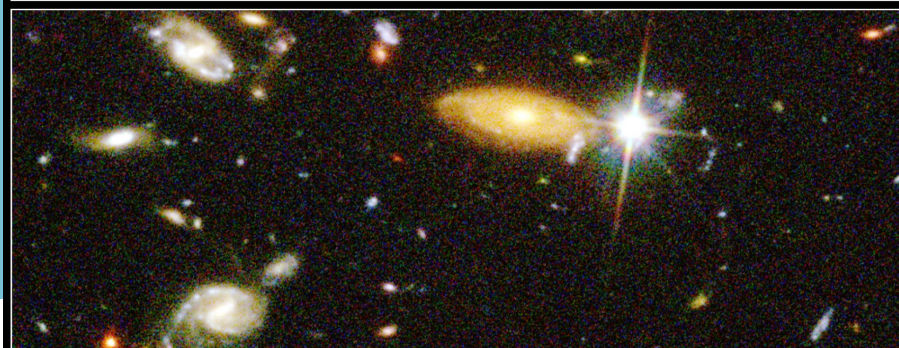
HST WFPC2

Ga



lution

I 2



**Hubble Deep Field Details • HST • WFPC2**



# Galaxy Formation and Evolution

Preliminary results from HDFs

- A multitude of faint galaxies is detected in these “blank” fields despite the relatively small areas covered (~3000 in HDF-N/S, ~10,000 in HUDF)

Preliminary results from HDFs

- A multitude of faint galaxies is detected in these “blank” fields despite the relatively small areas covered (~3000 in HDF-N/S, ~10,000 in HUDF)
- While the brighter (closer) galaxies have morphologies similar to those in the local Universe (e.g. E, SO, Sa,b,c), the fainter (more distant) galaxies often have distorted, irregular morphologies unlike nearby bright galaxies

- A multitude of faint galaxies is detected in these “blank” fields despite the relatively small areas covered (~3000 in HDF-N/S, ~10,000 in HUDF)
- While the brighter (closer) galaxies have morphologies similar to those in the local Universe (e.g. E, SO, Sa,b,c), the fainter (more distant) galaxies often have distorted, irregular morphologies unlike nearby bright galaxies
- Many of the most distant sources appear compact compared with nearby galaxies

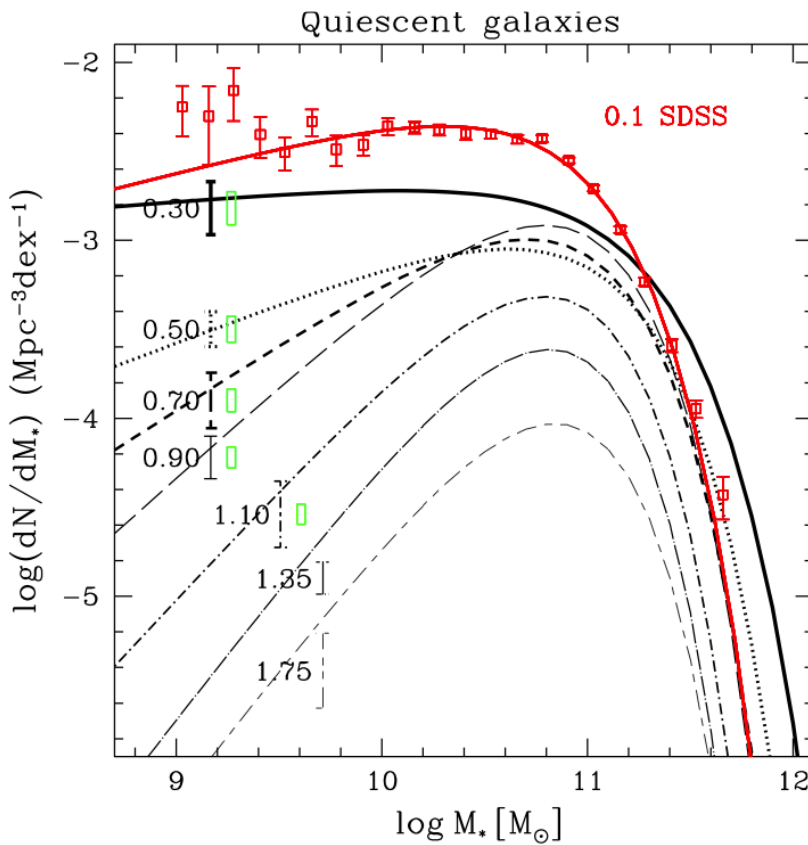
- A multitude of faint galaxies is detected in these “blank” fields despite the relatively small areas covered (~3000 in HDF-N/S, ~10,000 in HUDF)

(Galaxy Formation and Evolution  
Preliminary results from HDFS)

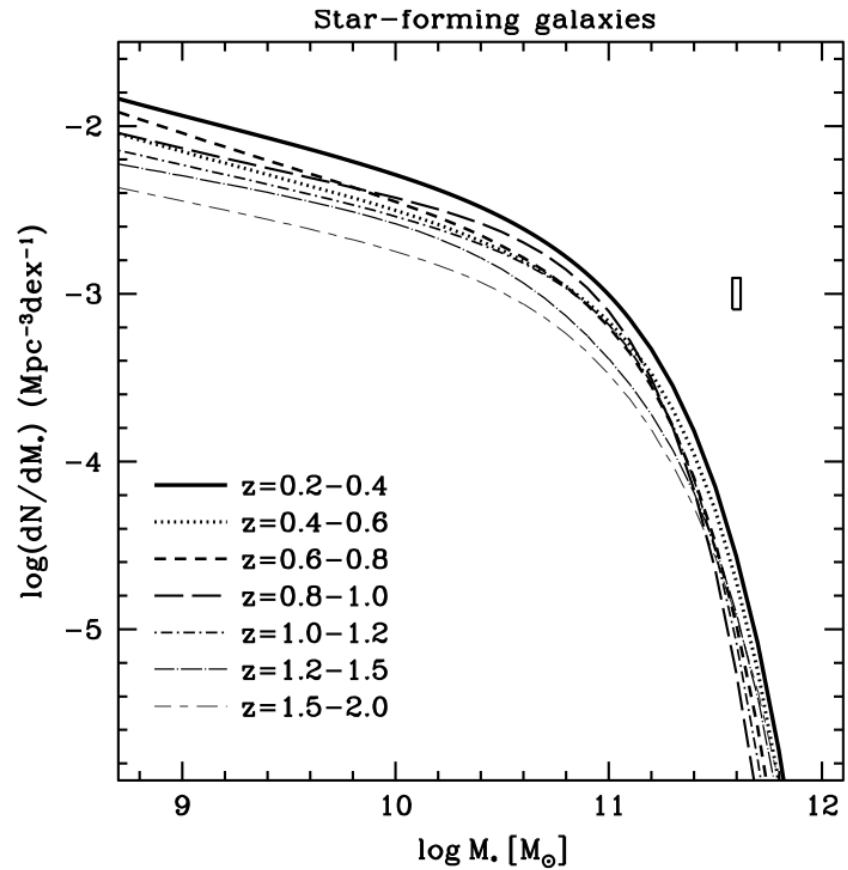
- While the brighter (closer) galaxies have morphologies similar to those in the local Universe (e.g. E, SO, Sa,b,c), the fainter (more distant) galaxies often have distorted, irregular morphologies unlike nearby bright galaxies
- Many of the most distant sources appear compact compared with nearby galaxies

results appear consistent with  
hierarchical galaxy evolution  
(small and grow through mergers)

# Some Key Science Results

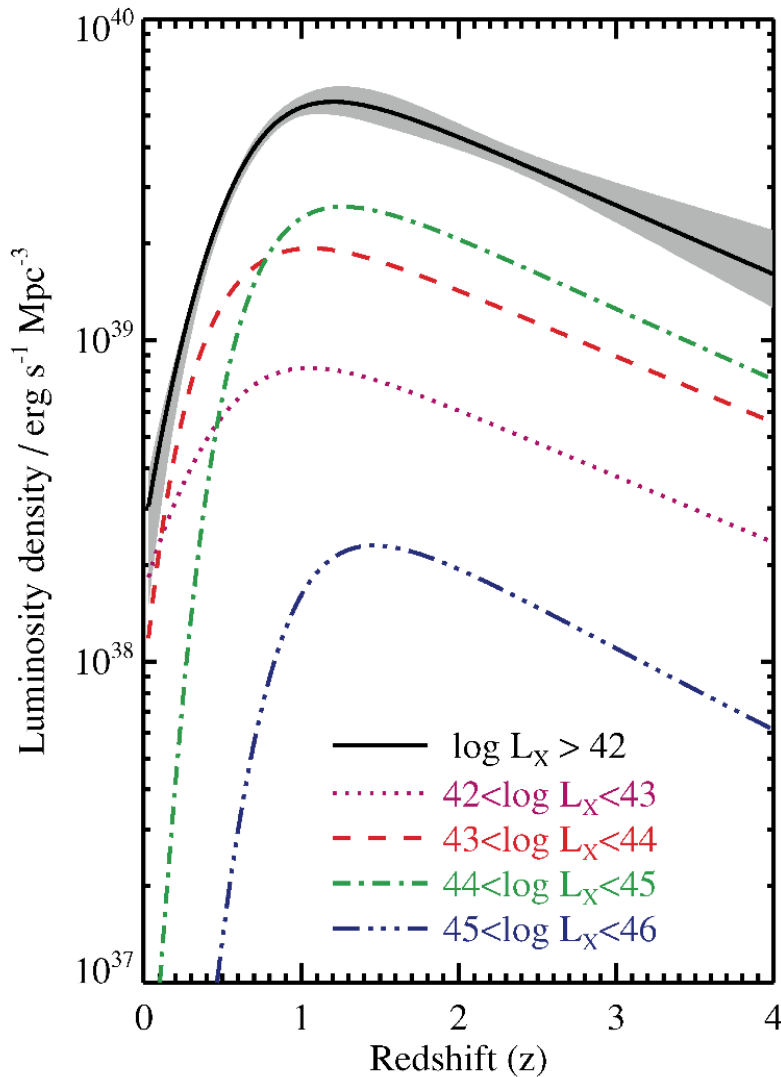


Evolution of the galaxy mass function.  
Downsizing: “Big galaxies formed first”.



# Some Key Science Results

## Black Hole accretion history



On average, black holes grew more rapidly in the early Universe.

BH “downsizing”: The most rapidly growing BHs dominated growth budget in the early Universe.